

Tracking the transition behavior and dynamics of ionic transport in crystalline ionic gel electrolytes†

HoSeok Park,^{ab} Se Ra Kwon,^b Young Mee Jung,^c Hoon Sik Kim,^d Hyun Joo Lee^e and Won Hi Hong^{*b}

Received (in Cambridge, UK) 29th May 2009, Accepted 8th September 2009

First published as an Advance Article on the web 24th September 2009

DOI: 10.1039/b910600f

The transition behavior and dynamics of ionic transport were strongly influenced by changes in the crystal structure and interaction field of the crystalline ionic gel electrolytes with respect to chemical compositions, as proven by impedance, ⁷Li NMR, PCA and 2D IR COS.

Intermolecular interactions of ionic materials with chemical environments are of fundamental importance for electrolytes, acid–base chemistry, supramolecular assembly, confinement, enzymatic proton transfer, biological systems, crystal engineering, *etc.*¹ In particular, stoichiometric ionic mixtures can reveal appealing phenomena, such as facilitated ionic transport and thermal transition due to the perturbed interaction fields.² The ionic interactions of ionic liquids (ILs) with other ionic compounds are known to strongly influence not only the structures and physicochemical properties of the IL itself,³ but also the geometry and force field of local circumstance.⁴ Despite extensive research, however, there are very few reports on the dynamics and transition behavior of ionic transport at certain discrete compositions because of the complexity and sensitivity of these systems.

ILs have become extremely attractive as a new type of highly efficient electrolyte, as well as environmentally benign solvents, due to non-volatility, low viscosity, low melting point, high boiling point, high ionic conductivity, thermal and electrochemical stabilities, and non-flammability.⁵ Furthermore, zwitter-type ionic liquids (ZILs), a new type of IL, have shown unique transport properties, such as an increased conductivity and transference number of the target ion.⁶ This is due to the complex secondary force field related to the intrinsic molecular structure, which is composed of covalently tethered cations and anions.⁶ Therefore, the transition behavior and dynamics of binary ionic mixtures, including ZILs and ionic salts, should be investigated.

The interactions and transport mechanisms of IL systems have been significantly investigated by a wide range of spectroscopic methods, such as UV-vis, IR, Raman and SFG spectroscopy,

NMR, and X-ray crystallography.⁷ However, it is very difficult to delicately track the transition of ionic transport under a specific environment, and to simultaneously monitor the dynamic process due to the overlapped bands and the restricted static information using one-dimensional (1D) spectroscopy. From this standpoint, two very popular and powerful techniques for spectroscopic studies are used herein: principal component analysis (PCA) and two-dimensional infrared correlation spectroscopy (2D IR COS). PCA gives a precise mathematical estimation of the changes along the sample and variable vectors.⁸ The 2D IR COS, which is generated by a cross-correlation analysis of dynamic fluctuations of IR signals induced by an external perturbation such as temperature, time, stress, concentration and others, is a well-established analytical technique to monitor the dynamic processes of complex systems.⁹

Herein, we first report the dynamics and transition behaviors of ion transport in binary crystalline ionic gel electrolytes consisting of 1-methylimidazolium-3-propanesulfonate (ImiZIL) and lithium bis(trifluorosulfonyl) amide (LiTFSI). Importantly, PCA is used to track the transition behavior of ionic conduction, while 2D IR COS is used to verify the dynamic process with respect to chemical compositions.

ImiZILs were synthesized following our previous procedure.¹⁰ Fig. 1 presents the ionic conductivities of binary ImiZIL-LiTFSI gel electrolytes as a function of temperature. The activation energies for lithium ion conduction of the ImiZIL-LiTFSI gel electrolyte were obtained from an Arrhenius plot. The ImiZIL-LiTFSI gel electrolyte showed an activation energy of 5.0 kJ mol⁻¹ at a molar ratio of 3 : 1, 3.3 kJ mol⁻¹ at a molar ratio of 2 : 1, 12.9 kJ mol⁻¹ at a molar ratio of 1 : 1,

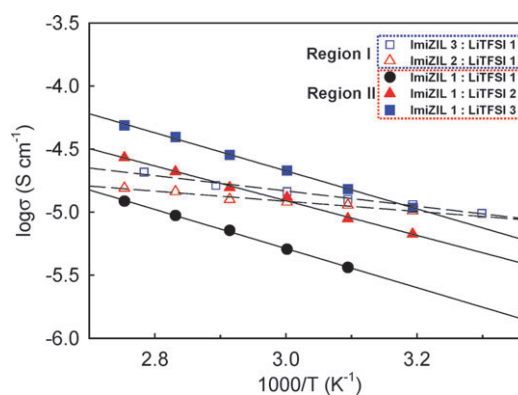


Fig. 1 Ionic conductivities of ImiZIL-LiTFSI mixtures as a function of temperature. The blue box indicates region I at the ImiZIL-rich phase, while the red box indicates region II at the LiTFSI-rich phase.

^a Department of Biological Engineering, Massachusetts Institute of Technology, 77 Massachusetts Ave., Cambridge, MA 02139, USA

^b Department of Chem. & Biomolecular Eng. (BK 21), KAIST, 335 Gwahagno, Yuseong-gu, Daejeon 305-701, Republic of Korea. E-mail: whhong@kaist.ac.kr; Tel: 82 42 350 3919

^c Department of Chemistry, Kangwon National University, Chunchon, 200-701, Korea

^d Department of Chemistry and Research Institute of Basic Sciences, Kyung Hee University, 1 Hoegidong, Dongdamoongu, Seoul, Korea

^e Division of Environment and Process Technology, KIST 39-1, Hawolgok-dong, Seongbuk-gu, Seoul 130-701, Korea

† Electronic supplementary information (ESI) available: Experimental section and additional characterization data. See DOI: 10.1039/b910600f

11.4 kJ mol⁻¹ at a molar ratio of 1 : 2, and 12.6 kJ mol⁻¹ at a molar ratio of 1 : 3. These values indicate the transport of lithium ions *via* a Grotthus-type mechanism. Despite the gel state of the binary mixture (see the ESI†), a plot of ionic conductivities matched with a linear Arrhenius behavior of the temperature-dependent conductivity better than the curved Vogel-Tamman-Fulcher (VTF) form, indicating ion hopping within the crystalline structures. When the content of ImiZIL was decreased below a molar ratio of 1 : 1, the ImiZIL-LiTFSI gel electrolyte showed 2–4-fold higher activation energies for the transport of lithium ions. Guided by different activation energies, the ionic conduction behaviors of binary gel electrolytes were divided into ImiZIL-rich phase in region I and LiTFSI-rich phase in region II. The existence of respective crystalline structures of ionic gel electrolytes at ImiZIL-rich and LiTFSI-rich phases indicates that the respective conduction behaviors in both regions I and II were derived from a structural arrangement by two molecular structures of binary gel electrolytes (see the ESI†).¹¹ Furthermore, in a similar manner to variations in the ionic conductivities and crystal structures, the simultaneous changes in the line widths and chemical shifts of the ⁷Li NMR spectra indicate the switch of the lithium ion conduction mechanism from region I to II with increasing concentration of LiTFSI (see ESI†).^{2a,12} In the view of force fields, ions in two crystal structures are surrounded by different neighboring hopping sites and interact with them through sequential conformational changes. Therefore, the transition of activation energies, crystal structures, chemical shifts, and ⁷Li line widths of the binary gel electrolyte elucidates that the transport of lithium ions occurred through respective conduction pathways due to different crystal structures and interaction fields.

The concentration-dependent IR spectra of the ImiZIL-LiTFSI mixture were obtained (see the ESI†). The representative bands regarding the imidazolium ring and sulfonate group of ImiZIL, and the TFSI anion of LiTFSI were particularly focused in the range of 1400 cm⁻¹–1000 cm⁻¹, because they are closely related to the transport properties. For the IR spectra of ImiZIL, in-plane ν C–H and twisting ν C–H of the imidazolium ring, and ν _aS=O of sulfonate group were assigned around 1170 cm⁻¹, 1130 cm⁻¹ and 1050 cm⁻¹, respectively. For the IR spectra of TFSI, in-phase ν _sS=O and ν _aS=O, and out-of-phase ν _sS=O and ν CF₃, were assigned around 1350 cm⁻¹, 1330 cm⁻¹, 1200 cm⁻¹ and 1100 cm⁻¹, respectively. Given that the band related to the sulfonate, imidazolium ring, and TFSI groups in the ImiZIL-LiTFSI system was shifted and weakened compared to that of the pristine ImiZIL, it was confirmed that conformational changes occurred *via* hydrogen bonding and/or electrostatic interactions.

PCA score and loading plots were obtained from the concentration-dependent FT-IR spectra to elucidate the dynamic transition of the ionic transport at a specific stoichiometry (Fig. 2). The score values of PC1 and PC2 clearly separate the FT-IR spectra into two regions. PC1 describes more than 91.9% of the total absorbance change of the spectra, whereas PC2 captures almost 7.4% of the remaining variances not described by PC1. In an analogous manner to the plots of ionic conductivities, crystal structures and ⁷Li line widths, PC1 exhibited turnover from negative to positive values at the molar ratio of 1 : 1. Considering that by definition the first PC corresponds to some physical phenomena related to the greatest amount of variation in the data,⁸ it is worth noting that the transition of transport properties

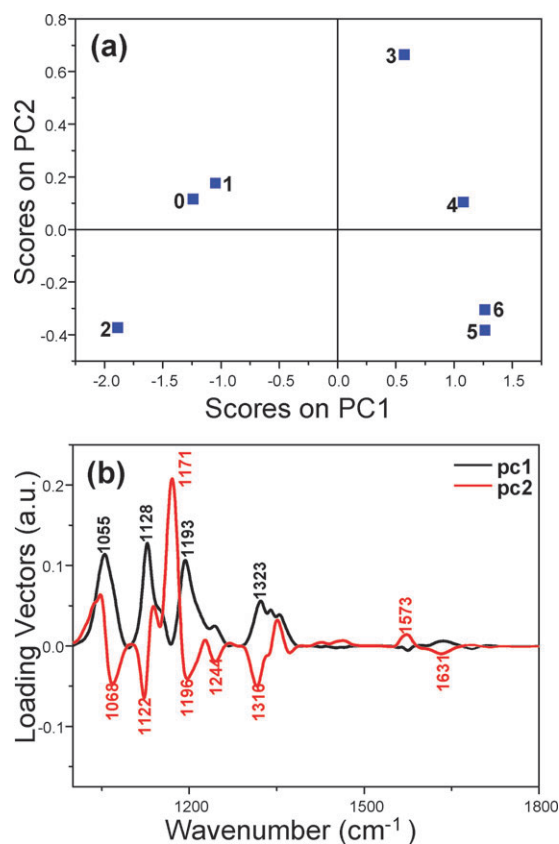


Fig. 2 (a) Scores and (b) loading vectors of PC1 (91.9 %) and PC2 (7.4 %) for the concentration-dependent FT-IR spectra of ImiZIL-LiTFSI mixtures. 0 indicates a molar ratio of ImiZIL-LiTFSI of 4 : 1, 1 of 3 : 1, 2 of 2 : 1, 3 of 1 : 1, 4 of 1 : 2, 5 of 1 : 3, and 6 of 1 : 4.

in ImiZIL-LiTFSI is strongly related to different dynamic processes of conformations in the two regions. This point is consistent with the transition of crystal structures and ⁷Li line widths from region I of the ImiZIL-rich phase to region II of the LiTFSI-rich phase. In particular, the observation of high positive PC1 loadings at 1323, 1193, 1128 and 1055 cm⁻¹ proves that the conformational changes in the imidazolium rings and sulfonate groups of ImiZILs and TFSI anions in LiTFSIs are responsible for the transition process of crystalline ionic gel electrolytes.

On the basis of tracking the transition point by PCA plots, the respective dynamic behaviors of the two regions were analyzed by 2D IR COS. Fig. 3 shows synchronous and asynchronous 2D correlation spectra of regions I and II. In a synchronous 2D correlation spectrum, the strong auto bands located at the diagonal positions represent the overall susceptibility of the corresponding spectral region to change in the spectral intensity as an external perturbation is applied to the system.⁹ The positions of the bands in the two sets of the power spectra are in good agreement with those detected by PC1. The emergence of an additional band at 1196 cm⁻¹ in region II and the unequal change in the absorption intensity are related to different dynamic behaviors. In particular, the synchronous 2D correlation spectrum for region II shows a four-leaf-clover cluster pattern, comprising two auto peaks at 1196 and 1170 cm⁻¹, and two negative cross peaks. The corresponding asynchronous 2D correlation spectrum reveals a very characteristic cluster pattern for the band position shift

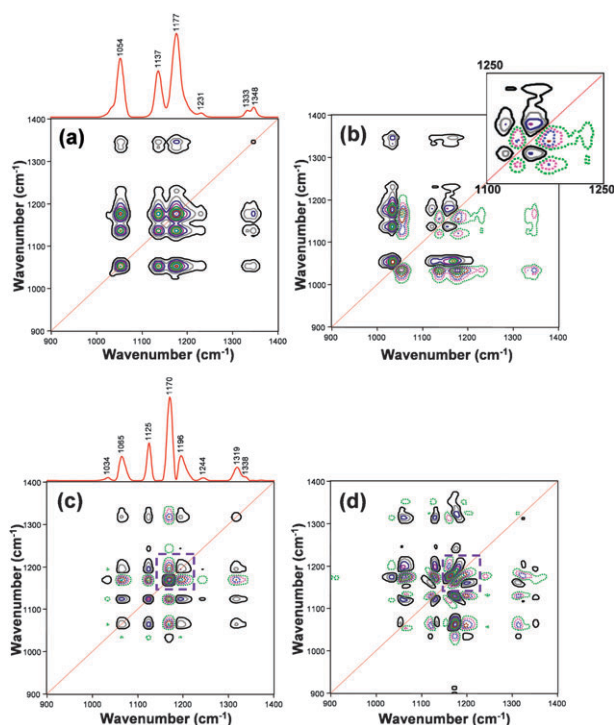


Fig. 3 (a) Synchronous and (b) asynchronous 2D correlation spectra of the ImiZIL-rich phase. The inset of (b) is the zoomed image in the range of 1100–1250 cm^{-1} . (c) Synchronous and (d) asynchronous 2D correlation spectra of the LiTFSI-rich phase.

due to the conformational changes, which is commonly known as the butterfly pattern. The interrelation of conformational changes attributed to the intermolecular interactions is derived from the cross bands located at off-diagonal positions of a synchronous 2D correlation spectrum, as it reveals simultaneous or coincidental changes of spectral intensities that are observed at two different spectral variables (ν_1 and ν_2).⁹ The positive cross bands at (1348, 1177) cm^{-1} , (1137, 1177) cm^{-1} and (1054, 1177) cm^{-1} in the synchronous 2D correlation spectrum in region I demonstrate that the change of spectral intensity at 1177 cm^{-1} is strongly interrelated with those at 1348 cm^{-1} , 1137 cm^{-1} and 1054 cm^{-1} . The conformational changes of the imidazolium rings were derived from those of the TFSI anions of LiTFSIs and/or the sulfonate groups of ImiZILs *via* hydrogen bonding. In the case of region II, one band near 1196 cm^{-1} reveals the same interrelation among conformations as region I, while the other band at 1170 cm^{-1} exhibits a reciprocal behavior of simultaneous spectra variation. It means that the dynamic behavior of the additional band in region II induces the mechanism of lithium ion conduction differently from that in region I, providing more complex interaction fields in the LiTFSI-rich phase.

In order to clarify different conduction mechanisms of the two regions, respective kinetics of conformational changes should be verified. Asynchronous 2D correlation spectra consisting of only cross bands provide information that is useful to interpret the kinetics of the chemical/physical reactions owing to the relative temporal relationship and the actual sequence of individual reaction processes.⁹ Consequently, an analysis of asynchronous 2D correlation in the two regions shows the following sequence of changes in spectral intensities by resolving overlapped bands: 1154, 1121, 1137, 1183

(imidazolium ring of ImiZIL) \rightarrow 1345 (TFSI anion of LiTFSI) \rightarrow 1056 (sulfonate group of ImiZIL) in region I and 1051 (sulfonate group of ImiZIL) \rightarrow 1130 (imidazolium ring of ImiZIL) \rightarrow 1065 (sulfonate group of ImiZIL) \rightarrow 1121 (imidazolium ring of ImiZIL) \rightarrow 1325, 1309 (TFSI anion of LiTFSI) in region II. Region I includes four different kinds of imidazolium rings and one kind of sulfonate group and TFSI anion, while region II has two different kinds of imidazolium rings and two kinds of sulfonate groups and TFSI anions. Therefore, significantly different variations of sequential spectra intensity in regions I and II confirm ion transport in respective dynamic environments created by two conduction pathways.

In summary, we have demonstrated the dynamics and transition behavior of lithium ion transport of binary crystalline ionic gel electrolytes due to the changes in the crystal structures and interaction fields. The analytical method suggested herein provides a useful and powerful way to capture the transition of physical, chemical, and biological properties and to monitor the dynamics in the complex system from a fundamental perspective.

We gratefully acknowledge Genome-based Integrated Bioprocess Project of the Ministry of Science and Technology of Korea.

Notes and references

- 1 A. C. Grimsdale and K. Müllen, *Angew. Chem., Int. Ed.*, 2005, **44**, 5592; T. N. G. Row, *Coord. Chem. Rev.*, 1999, **183**, 81; J. M. Lehn, *Supramolecular Chemistry: Concepts and Perspectives*, VCH, Weinheim, 1995; G. R. Desiraju, *Crystal Engineering: The Design of Organic Solids*, Elsevier, Amsterdam, 1989; C. B. Aakeröy and K. R. Seddon, *Chem. Soc. Rev.*, 1993, **22**, 397.
- 2 Z. Gadjourova, Y. G. Andreev, D. P. Tunstall and P. G. Bruce, *Nature*, 2001, **412**, 520; C. Zhang, Y. G. Andreev and P. G. Bruce, *Angew. Chem., Int. Ed.*, 2007, **46**, 2848; Y. Abu-Lebdeh, P.-J. Alarco and M. Armand, *Angew. Chem., Int. Ed.*, 2003, **42**, 4499; D. R. MacFarlane and M. Forsyth, *Adv. Mater.*, 2001, **13**, 957.
- 3 Y. Fukaya, K. Sekikawa, K. Murata, N. Nakamura and H. Ohno, *Chem. Commun.*, 2007, 3089; J. Wang, H. Wang, S. Zhang, H. Zhang and Y. Zhao, *J. Phys. Chem. B*, 2007, **111**, 6181.
- 4 I. Goodchild, L. Collier, S. L. Millar, I. Prokeš, J. C. D. Lord, C. P. Butts, J. Bowers, J. R. P. Webster and R. K. Heenan, *J. Colloid Interface Sci.*, 2007, **307**, 455; R. Atkin and G. G. Warr, *J. Phys. Chem. B*, 2007, **111**, 9309.
- 5 T. Welton, *Chem. Rev.*, 1999, **99**, 2071; J. Dupont, R. F. de Souza and P. A. Z. Suarez, *Chem. Rev.*, 2002, **102**, 3667; M. C. Buzzeo, R. G. Evans and R. G. Compton, *ChemPhysChem*, 2004, **5**, 1106; L. A. Blanchard, D. Hancu, E. J. Beckman and J. F. Brennecke, *Nature*, 1999, **399**, 28.
- 6 M. Yoshizawa, M. Hirao, K. Ito-Akita and H. Ohno, *J. Mater. Chem.*, 2001, **11**, 1057; C. Tiyapiboonchaiya, J. M. Pringle, J. Sun, N. Byrne, P. C. Howlett, D. R. MacFarlane and M. Forsyth, *Nat. Mater.*, 2004, **3**, 29; N. Byrne, P. C. Howlett, D. R. MacFarlane and M. Forsyth, *Adv. Mater.*, 2005, **17**, 2497.
- 7 T. Köddermann, C. Wertz, A. Heintz and R. Ludwig, *Angew. Chem., Int. Ed.*, 2006, **45**, 3697; S. Rivera-Rubero and S. Baldelli, *J. Am. Chem. Soc.*, 2004, **126**, 11788; Y. Zhao, S. Gao, J. Wang and J. Tang, *J. Phys. Chem. B*, 2008, **112**, 2031; A. Mele, C. D. Tran and S. H. D. Lacerda, *Angew. Chem., Int. Ed.*, 2003, **42**, 4364.
- 8 B. G. M. Vadegeinste, D. L. Massart, L. M. C. Buydens, S. De Jong, P. J. Lewi and J. Smeyers-Verbeke, *Handbook of Chemometrics and Qualimetrics: Part B*, Elsevier Science B. V., Amsterdam, The Netherlands, 1998, p. 88.
- 9 Y. Ozaki and I. Noda, *Two-Dimensional Correlation Spectroscopy: Applications in Vibrational Spectroscopy*, John Wiley & Sons, Inc., New York, 2004; I. Noda, *Appl. Spectrosc.*, 1993, **47**, 1329.
- 10 H. S. Kim, J. Y. Bae, S. J. Park, H. Lee, H. W. Bae, S. O. Kang, S. D. Lee and D. K. Choi, *Chem.-Eur. J.*, 2007, **13**, 2655.
- 11 E. Staunton, Y. G. Andreev and P. G. Bruce, *J. Am. Chem. Soc.*, 2005, **127**, 12176; A. M. Christie, S. J. Lilley, E. Staunton, Y. G. Andreev and P. G. Bruce, *Nature*, 2005, **433**, 50.
- 12 E. D. R. MacFarlane, J. Huang and M. Forsyth, *Nature*, 1999, **402**, 792.